Cell Communication and Signaling

RESEARCH

Open Access

Fractalkine/CX3CR1 axis is critical for neuroprotection induced by hypoxic postconditioning against cerebral ischemic injury

Lixuan Zhan[1†], Meiqian Qiu[1†], Jianhua Zheng[1], Meijing Lai[1], Kunqin Lin[1], Jiahua Dai[1], Weiwen Sun[1] and En Xu[1*]

Abstract

Microglial activation-mediated neuroinflammation is a major contributor to neuronal damage after cerebral ischemia. The Fractalkine (FKN)/CX3C chemokine receptor 1 (CX3CR1) axis plays a critical role in regulating microglial activation and neuroinflammation. The aim of this study is to ascertain the role and mechanism of FKN/CX3CR1 axis in hypoxic postconditioning (HPC)-induced anti-inflammatory and neuroprotective effects on transient global cerebral ischemia (tGCI). We found that HPC suppressed microglial activation and alleviated neuroinflammation in hippocampal CA1 after tGCI. Meanwhile, HPC upregulated the expression of FKN and CX3CR1 in neurons, but it downregulated the expression of CX3CR1 in glial cells after tGCI. In addition, the overexpression of FKN induced by the administration of FKN-carried lentivirus reduced microglial activation and inhibited neuroinflammation in CA1 after tGCI. Furthermore, silencing CX3CR1 with CX3CRi-carried lentivirus in CA1 after tGCI suppressed microglial activation and neuroinflammation and exerted neuroprotective effects. Finally, the overexpression of FKN caused a marked increase of neuronal CX3CR1 receptors, upregulated the phosphorylation of Akt, and reduced neuronal loss of rats in CA1 after tGCI. These findings demonstrated that HPC protected against neuronal damage in CA1 of tGCI rats through inhibiting microglial activation and activating Akt signaling pathway *via* FKN/CX3CR1 axis.

Keywords Fractalkine, CX3CR1, Neuroinflammation, Akt, Cerebral ischemia, Hypoxic postconditioning

Introduction

The brain damage due to cerebral ischemia is a leading cause of morbidity and mortality worldwide. Transient global cerebral ischemia (tGCI) that results from cardiac arrest, severe hypotension and coronary artery bypass, leads to the selective and delayed neuronal injury of the hippocampal cornu amonis (CA) 1 region [1]. It is now widely known that cerebral ischemia triggers a widespread inflammatory reaction, which significant contributes to ischemia-induced neuronal death. Inflammation driven primarily by activating glial cells that reside in the central nervous system (CNS) produces several

†Lixuan Zhan and Meiqian Qiu contributed equally to this work.

*Correspondence:
En Xu
enxu@163.net
[1]Department of Neurology, Institute of Neuroscience, Key Laboratory of Neurogenetics and Channelopathies of Guangdong Province and the Ministry of Education of China, The Second Affiliated Hospital, Guangzhou Medical University, 250 Changgang Dong RD, Guangzhou 510260, P. R. China

proinflammatory factors, such as tumor necrosis factor (TNF)-α and interleukin (IL)-1β, which lead to a disruption of cellular homeostasis and structural damage of brain. Microglia, the resident immune cells of the brain, play pivotal roles in inflammatory responses after cerebral ischemia. During brain ischemia, microglia are activated, as shown by process thickening and hypertrophy of the cell body, with coinciding upregulation of cell surface markers, such as cluster of differentiation (CD) 68 [2–4]. A large body of data shows that anti-inflammatory drugs that inhibit the activation of microglia serve to protect against cerebral ischemia-induced insults to the CNS [5, 6]. Our previous study demonstrated that hypoxic postconditioning (HPC) with 8% O_2 for 120 min protects hippocampal CA1 pyramidal neurons against tGCI injury in adult rats [7]. Even so, what remains unknown is whether HPC exerts neuroprotection against tGCI-induced injury by modulating microglia-mediated inflammation.

The established consensus is that the mechanism of microglial activation during cerebral ischemia involves multiple pathways. It is noteworthy that Fractalkine (FKN)/CX3C chemokine receptor 1 (CX3CR1) axis mediates microglia-neuron communications, either in physiological or pathological states [4, 8, 9], involving in the microglial activation. As the only member of the CX3C chemokine family, FKN exists in the form of membrane-anchored FKN (mFKN) and soluble FKN (sFKN) isoforms. The former consists of an extracellular N-terminal domain, a mucin-like stalk domain connecting with the cell membrane, a transmembrane domain and an intracellular C-terminal domain. Extracellular domain of mFKN can be cleaved into sFKN. Subsequently FKN binds to its only identified receptor, CX3CR1 and initiates its downstream signal pathway [10–13]. Under normal conditions, microglia are kept quiescent through FKN/CX3CR1 cross-communication between neurons and glial cells. Rather, the disruption of FKN/CX3CR1 axis can result in microglial activation and overexpression of TNF-α and IL-1β [4]. Although growing body of evidence suggests the involvement of FKN/CX3CR1 axis in brain disorders, the published results are relatively controversial. For example, the neuroprotective role for FKN/CX3CR1 has been supported in studies of amyotrophic lateral sclerosis [14], Parkinson's disease [15–17] and multiple sclerosis in some studies [18], whereas a neurotoxic role for FKN/CX3CR1 has been demonstrated in Alzheimer's disease [19, 20] and stroke [21] in another. The controversial results indicate that a disruption of FKN/CX3CR1 axis can induce a disease-specific microglial response which can be regarded as either beneficial or detrimental. Thus, it follows that, the ascertained roles of FKN/CX3CR1 shall shed light on the ischemic tolerance induced by HPC after tGCI.

In general, FKN predominantly expresses on neurons in CNS, whereas CX3CR1 is thought to be restricted to microglia [22, 23], and contributes to the chemoattraction processes and the activation of microglia following neuroinflammation or brain injury [24]. Although increasing evidence suggests that astrocytes and hippocampal neurons express CX3CR1 [25–29], less established is the role of the astrocytic and neuronal CX3CR1. Intriguingly, FKN directly modulates neuronal survival *via* autoregulatory interaction [28], which means, it can be released from these neurons, possibly by interacting directly with its receptor expressed on the same cell. FKN is proposed to protect hippocampal neurons from the neurotoxicity through activation of protein kinase B [28], also known as Akt, an important component of prosurvival and antiapoptotic mechanism in neurons [30, 31]. Notably, our prior study has revealed that HPC increased phosphorylation of Akt in CA1 after tGCI, while the inhibition of Akt phosphorylation with LY294002 suppressed the neuroprotection induced by HPC. Our results supported that the activation of Akt signaling pathway mediated by HPC contributed to the induction of neuroprotection against tGCI [7]. This led us to the investigation of whether FKN/CX3CR1 axis activated Akt signaling pathway to mediate HPC-induced neuroprotection against tGCI.

In the current study, we intend to explore the roles of FKN/CX3CR1 axis in HPC-induced neuroprotection against tGCI. We also directed our efforts to the potential molecular mechanism of FKN/CX3CR1 axis in microglia-mediated neuroinflammation after tGCI and in neuronal survival modulated *via* activation of Akt signaling pathway after HPC.

Materials and methods

Animals

Animal experimental procedures were carried out according to the Animal Research: Reporting In Vivo Experiments guidelines under the oversight of the Animals Care and Use Committee of Guangzhou Medical University (Guangzhou, China). Adult male Wistar rats weighing 220–280 g (aged 7–8 weeks) were used and obtained from Southern Medical University (Guangzhou, China). All animals were free to access food and water, and were housed under a temperature-controlled environment (21–23 ℃) on a 12 h light-dark cycle. According to the standard procedures, rats were randomly divided into different groups using a random number table.

Transient global cerebral ischemia and hypoxic postconditioning

Transient global cerebral ischemia in tGCI group was induced in accordance with the four-vessel occlusion method [32]. In brief, the animals were anesthetized with

3–4% isoflurane in a chamber. Anesthesia was maintained with a mask using 2–3% isoflurane during the operation. Bilateral vertebral arteries were blocked by electrocauterization. Common carotid arteries were isolated, and a teflon/silastic occluding device was placed around each common carotid artery without interrupting blood flow. Twenty-four hours after surgery, global cerebral ischemia was induced in the awake rats for 10 min by occluding both common carotid arteries. After occlusion, rats that lost their righting reflex within 1 min and had mydriasis were selected for later experiments. Rectal temperature was maintained at a temperature of 37–38 ℃ throughout the experiments. The rats in Sham-operated (Sham) group received the same surgical procedures without 10-min occlusion of common carotid arteries. All operations were performed under aseptic conditions. In HPC group, rats were placed in a hypoxic chamber with air containing 8% O_2 and 92% N_2 flowing continuously at 23–25 ℃ for 120 min at 24 h after ischemia. Twenty-four hours after sham-operated procedures without ischemia, sham-operated, hypoxia-treated rats (hereinafter referred to as hypoxia group) were exposed to 120-min hypoxia. The experimental schedule is shown in Suppl Fig. S1.

Immunohistochemistry

Rats were sacrificed at 0, 4, 26 and 50 h after reperfusion with or without hypoxia, respectively, and samples were prepared as described previously [33]. Single-label immunohistochemistry was performed using avidin-biotin-peroxidase complex (ABC) method, as previously mentioned [34]. In brief, the sections were first soaked in 3% hydrogen peroxide for 30 min, followed by 5% normal serum for 1 h at room temperature, and then incubated with primary antibodies overnight at 4 ℃. The primary antibodies used included mouse anti-Iba-1 (ionized calcium binding adaptor molecule-1; 1:200; Cat#019-19741, Wako), mouse anti-CD68 (1:200; Cat# MAB1435, MilliporeSigma), rabbit anti-mFKN (1:300; Cat# ab25088, Abcam), rabbit anti-CX3CR1 (1:3000; Cat# ab8021, Abcam) and mouse anti-NeuN (neuronal nuclei; 1:4000; Cat# Mab377, MilliporeSigma). After being washed with phosphate-buffered saline (PBS), the sections were incubated with biotinylated secondary immunoglobulin G (IgG) antibody for 2 h, and then treated with ABC for 30 min at room temperature. The peroxidase reaction was visualized with 0.05% diaminobenzidine and 0.01% hydrogen peroxide. The number or the optical density of immunopositive cells was quantified from 4 nonrepeated random fields of 0.037 mm^2 in CA1 under a light microscope with ×660 magnification. Data were quantified bilaterally in 4 sections from each rat and assessed blindedly.

Double-fluorescent immunohistochemistry was performed to observe cell types and the exact position where mFKN and CX3CR1 were distributed. NeuN, glial fibrillary acidic protein (GFAP) and Iba-1 were used to identify neuronal nuclei, astrocytes and microglia, respectively. Antibodies used in these studies included rabbit anti-mFKN (1:50; Cat# ab25088, Abcam), rabbit anti-CX3CR1 (1:3000; Cat# ab8021, Abcam; 1:200; Cat#13885-1-AP, Proteintech), mouse anti-CX3CR1 (1:50; Cat# 824002, Biolegend), mouse anti-NeuN (1:1000; Cat# MAB377, MilliporeSigma), rabbit anti-NeuN (1:1000; Cat# ABN78, MilliporeSigma), mouse anti-GFAP (1:3000; Cat# AMB360, MilliporeSigma), rabbit anti-GFAP (1:3000, Cat# AB5804, MilliporeSigma), mouse anti-Iba-1 (1:500, Cat# 234 011, Synaptic Systems), rabbit anti-Iba-1 (1:10000; Cat# 019-19741 Wako), Cy3-conjugated goat anti-mouse IgG antibody (1:100; Cat# AP124C, MilliporeSigma), Alexa Fluor 488-conjugated goat anti-mouse antibody (1:100; Cat# ab150077, Abcam), Cy3-conjugated goat anti-rabbit IgG antibody (1:100; Cat# AP132C, MilliporeSigma), and Alexa Fluor 488-conjugated goat anti-rabbit antibody (1:100; Cat# ab150077, Abcam). Slides were analyzed with a confocal laser microscope (SP8, Leica Microsystems, Wetzlar, Hessen, Germany). Colocalization was quantified by Pearson's coefficient and Mander's coefficient with Costes threshold using FIJI/ImageJ coloc2 plugin.

Fluorescence in situ hybridization assay

The Cy3-labeled probes specific to targeting rat CX3CR1 were designed and synthesized by GenePharma (Shanghai, China), and the fluorescence in situ hybridization (FISH) assay was performed using a fluorescence in situ hybridization kit (GenePharma, Shanghai, China) following the manufacturer's instructions. The images were acquired and analyzed with a confocal microscopy system (SP8, Leica Microsystems). The probe sequences are shown below: 5′-tagataggaagatggtcccaaccagaccgaacgtgaagaccaaagagcaggtcgctcaag-3′.

Western blotting

The animals were euthanized at 0, 4, 26, and 50 h after reperfusion with or without hypoxia, respectively. The brain tissue was cut into 2 mm coronal slices using a brain matrix, and the CA1 subregions of bilateral hippocampi were quickly dissected under a stereomicroscope. Proteins of CA1 were extracted and Western blotting procedure was performed as described previously [34]. Protein concentration was detected by bicinchoninic acid method recommended by the manufacturer (Beyotime, Jiangsu, China). The proteins were separated by sodium dodecyl sulfate-polyacrylamide gel electrophoresis and then transferred to polyvinylidene fluoride membranes (MilliporeSigma). The primary antibodies included

rabbit anti-mFKN (1:1000; Cat# ab25088, Abcam), rabbit anti-sFKN (1:4000; Cat# ab25088, Abcam), rabbit anti-CX3CR1 (1:1000, Cat# ab8021, Abcam), mouse anti-glyceraldehyde 3-phosphate dehydrogenase (GADPH) (1:10000; Cat# 60004-I-Ig, Proteintech), rabbit anti-Akt (1:8000; Cat# 4685 S, Cell Signaling Technology), and rabbit anti-p-Akt (1:1000; Cat# 4060 S, Cell Signaling Technology). The intensity of each band was quantified with ImageJ software, calibrated with the housekeeping protein GAPDH, and was normalized to those in Sham rats.

Lentivirus construction and administration

Plasmids containing the sequence of rat *FKN* (GenBank accession number NM_134455) and a negative control (NC) sequence (CON319) were designed by Genechem (Shanghai, China). In brief, the sequence was inserted into *Age*I and *Age*I sites of the Ubi-MCS-3FLAG-CMV-EGFP (GV365) lentiviral vector. To produce recombinant lentiviruses, the shuttle vector and viral packaging system were cotransfected into HEK293T cells using Lipofectamine 2000 (Invitrogen, San Diego, CA, USA). Afterwards, HEK293T cells were used for viral infection. The infection efficiency monitored with GFP protein expression was greater than 80%. After 48 h of infection, cells were harvested and total RNA were extracted to examine the mRNA expression of FKN. The titers of lentiviruses were approximately 5×10^8 TU/ml. A total of 5 μl volume (1.25 μl virus diluted by 3.75 μl enhanced solution) containing 0.625×10^6 TU of particles was injected into the bilateral CA1 region (3.5 mm posterior to bregma, 2.3 mm lateral to bregma, and 2.6 mm below the dura) using the RWD syringe and WPI infusion pump at a speed of 30 μl/h.

Three small-interfering RNA sequences targeted rat *CX3CR1* (Genbank accession number NM_133534) and a NC vector (CON208) were designed by Genechem. The sequences for *CX3CR1*-RNAi 1, 2, 3 were GTCCA AGAGCATCACTGACAT, GGCCGCCAACTCCATGA ACAA, and AGCCATTAGGCTCATCCTCTT, respectively. Briefly, RNAi was inserted into *Age*I and *EcoR*I sites of the hU6-MCS-Ubiquitin-EGFP-IRES-puromycin (GV248) lentiviral vector. The shuttle vector and viral packaging system were contransfected into HEK293T to produce recombinant lentiviral particles. To verify inhibition efficacy, lentiviral particles were transferred into rat Schwann cell line RSC96, CX3CR1 mRNA expression levels were examined by RT-qPCR. The results showed that the best-performing *CX3CR1*-RNAi sequence was GTCCAAGAGCATCACTGACAT (*CX3CR1*-RNAi 1) with maximal inhibitory efficacy. Therefore, *CX3CR1*-RNAi 1 was utilized for subsequent experiments. Titers of lentiviral particles were approximately 8×10^8 TU/ml. Accordingly, a 5-μl volume containing 1.25×10^6 TU of particles was bilaterally injected into CA1.

Rats were allowed to recover for up to 14 d after lentiviral injection to ensure sufficient gene expression before being used for subsequent experiment.

Analysis of cell viability

As done previously, Nissl and NeuN staining were performed to verify the hippocampal cell viability after 168 h of reperfusion. Sections from Nissl and NeuN staining were examined under a light microscope (×660), and cell counts were conducted [35]. Cells in the CA1 pyramidal layer were quantitatively analyzed within three non-repeated rectangular areas of 0.037 mm^2 in the typical dorsal hippocampus (between anterior-posterior (AP) 4.8 and 5.8 mm, interaural or AP 3.3–3.4 mm, bregma). Data were quantified bilaterally in sections from each brain and assessed blindedly, and four sections per animal were evaluated.

Statistical analysis

Statistical data analyses were performed using Statistical Package for Social Sciences Software for Windows, version 25.0 (SPSS, Inc., Chicago, IL, USA). All data were checked by normal distribution and homogeneity of variance, respectively. When the data were normally distributed, one-way ANOVA and *t*-test were applied. For comparison between the two groups, the student two-tailed t-test was performed. Multiple comparisons were performed by using one-way ANOVA followed by Least Significant Difference (LSD) test for comparisons of Sham versus tGCI at different time points, or ANOVA followed by Bonferroni's test for comparisons the significant difference at different time points in tGCI or HPC groups. When the data were normally distributed and the variances were unequal, multiple comparisons were conducted by using one-way ANOVA followed by Tamhane's T2 post-hoc test. When the data were abnormally distributed and the variances were unequal, nonparametric tests were used, including Mann-Whitney's U test for the comparison between two groups and Kruskal-Wallis for multiple comparisons. Data were expressed as the mean ± standard deviation (SD). Differences were considered statistically significant when $p<0.05$. All data graphing were performed using the GraphPad Prism 6 software (GraphPad, La Jolla, CA).

Results

HPC inhibits microglial activation and attenuates neuroinflammation in CA1 after tGCI

To ascertain whether HPC inhibits microglial activation in CA1 after tGCI, the expression of Iba-1 and CD68 in CA1 was examined with immunohistochemical assay. We used CD68, a specific marker for the transmembrane

glycoprotein localized within lysosomal membranes as an index of typical microglia based on shape and size of the soma [36, 37]. Iba-1-positive cells in CA1 of Sham rats showed classical ramified morphology, with a small cell soma and fine processes (Fig. 1A, a-b). However, at 168 h of reperfusion, Iba-1-positive cells in CA1 of tGCI or HPC rats displayed typical activated morphology, with retracting and thickening of processes and hypertrophy of cell body (Fig. 1A, c-f). Compared with Sham group, statistical analysis did not reveal a significant effect of hypoxia on the number of Iba-1-positive in CA1 of Sham rats. However, the number of Iba-1-positive

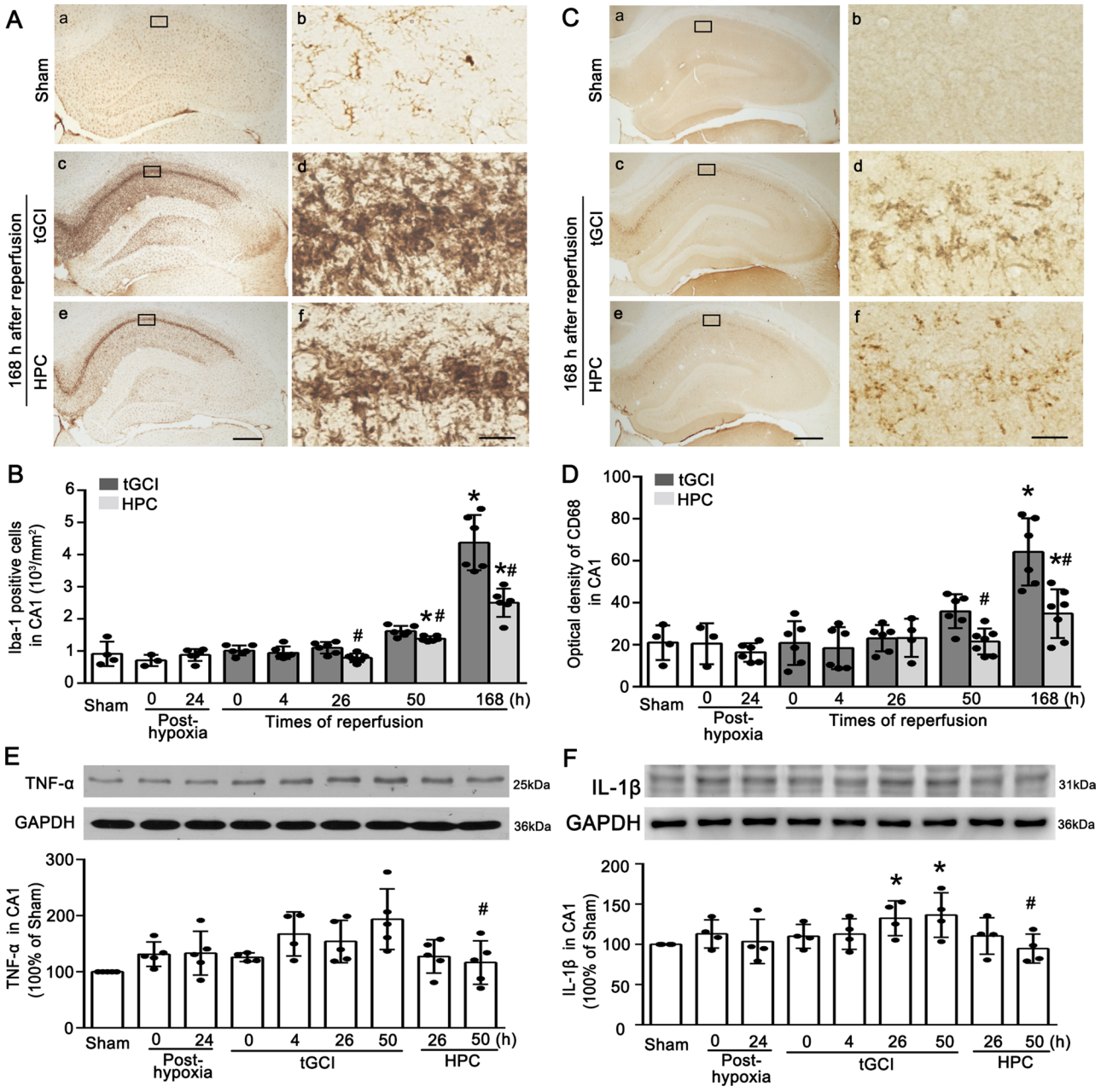

Fig. 1 HPC prevents the activation of microglia and alleviates inflammatory response in CA1 after tGCI. (**A**) Immunohistochemistry of Iba-1 in rat brains. Representative images show Sham group (a, b), 168 h after reperfusion of tGCI groups (c, d) and HPC groups (e, f), respectively. Scale bar, 250 μm (a, c, e) and 25 μm (b, d, f). (**B**) Quantitative analyses of Iba-1-positive cells in CA1. (**C**) Immunohistochemistry of CD68 in rat brains. Representative images show Sham group (a, b), 168 h after reperfusion of tGCI groups (c, d) and HPC groups (e, f), respectively. Scale bar, 250 μm (a, c, e) and 25 μm (b, d, f). (**D**) Quantitative analyses of CD68-immunoreactivities in CA1. (**E**, **F**) Representative immunoblots showing the expressions of TNF-α and IL-1β in CA1, respectively. The histogram presents the quantitative analyses of TNF-α and IL-1β levels. The horizontal axis of the chart represents times of reoxygenation or reperfusion. Data are expressed as percentage of value of Sham animals. Each bar represents the mean ± S.D. *$p < 0.05$ vs. Sham animals and #$p < 0.05$ vs. tGCI groups at the same time point

cells significantly increased at 168 h after tGCI. HPC decreased the number of Iba-1-positive cells at 26–168 h after tGCI (Fig. 1B). As expected, the expression pattern of CD68 was similar to that of Iba-1 in CA1. Similarly, hypoxia did not affect the expression of CD68 in CA1 of Sham rats, but HPC significantly reduced the expression of CD68 at 50 h and 168 h after tGCI (Fig. 1C-D). These results suggest that HPC can suppress the activation of microglia after tGCI.

Subsequently, we examined the protein expression of inflammatory cytokines TNF-α and IL-1β in CA1 with Western blotting. As shown in Fig. 1E and F, no differences were observed regarding both levels of TNF-α and IL-1β in CA1 of hypoxia groups. By contrast, HPC reduced the expression of TNF-α in CA1 at 50 h after tGCI (Fig. 1E). Similarly, IL-1β was increased at 26 h and 50 h after reperfusion of tGCI, while HPC repressed this increase of IL-1β at 50 h after reperfusion (Fig. 1F).

HPC inhibits microglial activation via upregulating FKN in CA1 after tGCI

To ascertain the underlying mechanism by which HPC inhibits microglial activation after tGCI, the expression of FKN in CA1 was examined using immunohistochemical assay and Western blotting. The results showed a high expression of mFKN in CA1 of Sham, and that mFKN-positive cells mainly existed in the neuron-like cells of pyramidal layer of hippocampus either in tGCI or HPC groups (Fig. 2A). The quantitative analysis of mFKN immunopositive cells in CA1, as shown in Fig. 2B, revealed that the number of mFKN-positive cells both in hypoxia and tGCI groups decreased at 26–168 h after reperfusion, compared with the Sham group. Strikingly, HPC prevented this reduction induced by tGCI at 26–168 h. Also, the changes in mFKN level were further confirmed by Western blotting analysis, in which the expression of mFKN in CA1 decreased at 0 h after hypoxia and at 0–50 h after tGCI, and HPC increased mFKN expression at 26 h and 50 h after reperfusion (Fig. 2C). In contrast, the expression of sFKN in CA1 of tGCI rats upregulated at 26 h after reperfusion. On the other hand, HPC exerted no significant effect on the expression of sFKN after tGCI. Double-fluorescent immunohistochemistry was performed to ascertain cell types expressing mFKN in CA1 after tGCI with or without hypoxia, which revealed that mFKN was colocalized with neuronal marker protein NeuN in Sham and tGCI rats at 168 h after reperfusion with or without hypoxia (Fig. 2D), indicating that mKFN was predominantly localized in neurons.

To further ascertain the extent to which HPC inhibited microglial activation and neuroinflammation via upregulating FKN in CA1 after tGCI, FKN-carried lentivirus (referred to as OE-*FKN*) was administrated into the bilateral hippocampus. Rats were randomly subjected to Sham operation, or tGCI with or without hypoxia 14 days after the administration of OE-*FKN* or scrambled lentivirus vector (referred to as LV-con) (Fig. 3A). The effectiveness of lentivirus transfection was verified as shown in Fig. 3B-C. As shown by immunofluorescence, mFKN was colocalized with GFP in OE-*FKN* administrated rats at 7 days after tGCI (Fig. 3C). In addition, mFKN expression in CA1 detected by Western blotting increased both in Sham and tGCI rats after OE-*FKN* administrated at 50 h of reperfusion (Fig. 3D). Meanwhile, OE-*FKN* administration prevented increase in the expressions of TNF-α and IL-1β in CA1 after tGCI (Fig. 3E-F). Accordingly, we examined the effects of OE-*FKN* administration on microglial activation in CA1 after tGCI with or without hypoxia at 7 days of reperfusion. As shown in Fig. 3G-I, the number of Iba-1-positive cells and the optical density of CD68 were markedly reduced in tGCI rats after OE-*FKN* administration, indicating that the overexpression of FKN in CA1 mediated by FKN-carried lentivirus mimics the neuroprotective effects of HPC against tGCI.

HPC exerts neuroprotective effects by upregulating CX3CR1 in neurons and downregulating CX3CR1 in glial cells in CA1 after tGCI

Since FKN is capable of suppressing activation of microglia and attenuating inflammation by binding with the specific receptor CX3CR1, we examined the expression of CX3CR1 in CA1 of rats exposed to tGCI with or without hypoxia. Immunohistochemical assay showed that CX3CR1-positive cells mainly existed in the pyramidal cell layer with neuron-like appearance in Sham, tGCI rats at the early reperfusion and HPC groups (Fig. 4A, a-d, g, h). Notably, at 168 h after tGCI, CX3CR1 was expressed mainly in cells with glia-like appearance, which exhibited polymorphic somata and processes (Fig. 4A, e, f). The quantitative analysis showed that compared with Sham group, the number of CX3CR1-positive cells increased at 24 h after reoxygenation in hypoxia groups, and at 0–50 h after reperfusion of tGCI. However, when compared with tGCI rats, the number of CX3CR1-positive cells in HPC rats showed a slightly increase at 26 h but a slightly decrease at 168 h (Fig. 4B). Interestingly, compared with Sham group, the number of CX3CR1-positive glia-like cells in CA1 were largely increased both in hypoxia groups and tGCI groups after reperfusion at 50 h and 168 h. On the other hand, HPC reduced the number of CX3CR1-positive glia-like cells at 50 h and 168 h after reperfusion (Fig. 4C). Meanwhile, the number of CX3CR1-positive neuron-like cells in CA1 increased at 0–26 h, and then significantly decreased at 50 h and 168 h after reperfusion of tGCI. Hypoxia did not affect the number of CX3CR1-positive neuron-like cells in CA1 of Sham rats. In contrast, HPC repressed the reduction

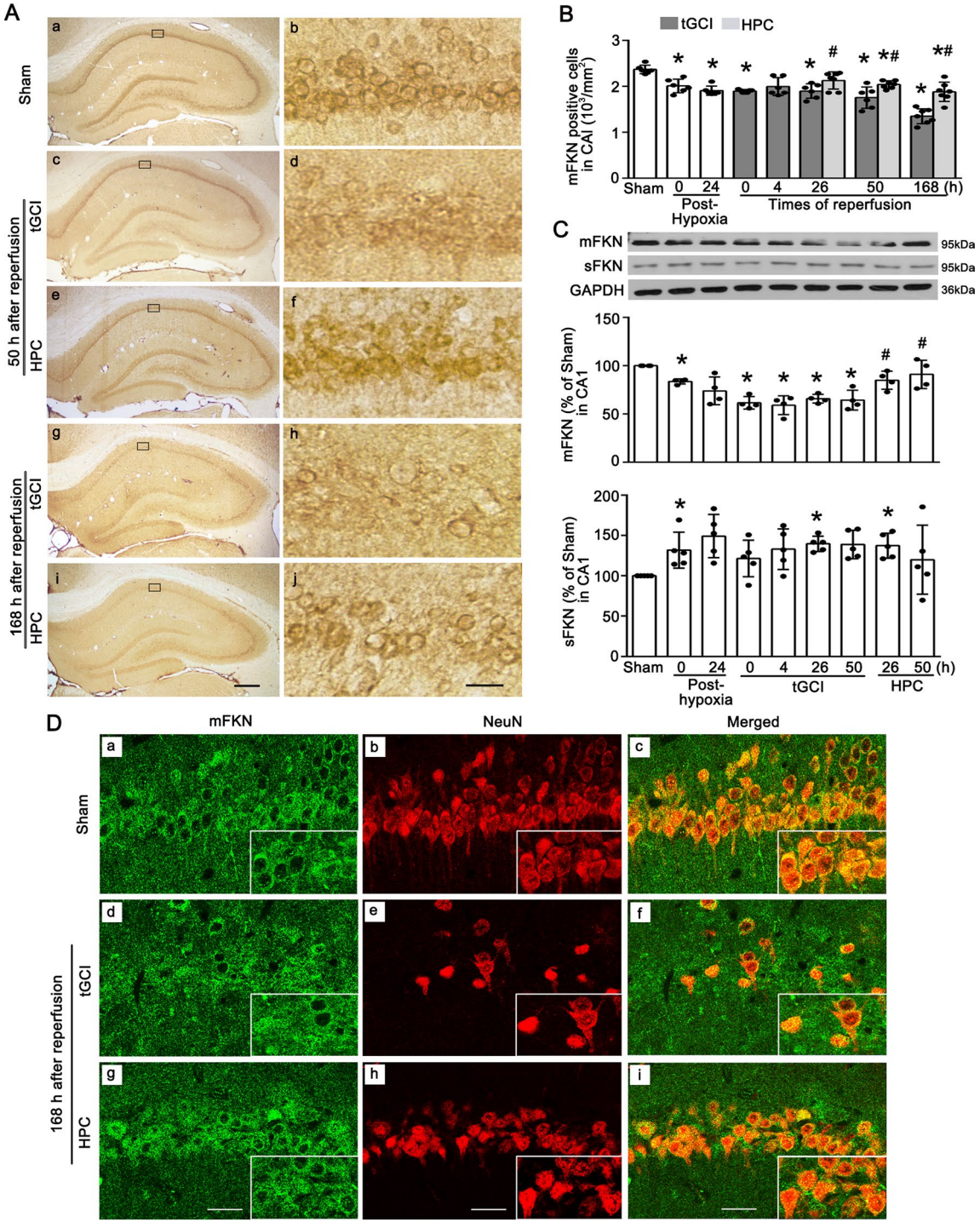

Fig. 2 The effects of HPC on the expression of mFKN and sFKN in CA1 after tGCI. (**A**) Immunohistochemistry of mFKN in rat brains. Representative images show Sham group (a, b), 50 h after reperfusion of tGCI groups (c, d) and HPC groups (e, f), 168 h after reperfusion of tGCI groups (g, h) and HPC groups (i, j), respectively. Scale bar, 250 μm (a, c, e, g, i) and 25 μm (b, d, f, h, j). (**B**) Quantitative analyses of mFKN-positive cells in CA1. (**C**) Representative immunoblots showing the expressions of mFKN and sFKN in CA1, respectively. The histogram presents the quantitative analyses of mFKN and sFKN levels. The horizontal axis of the chart represents times of reoxygenation or reperfusion. Data are expressed as percentage of value of Sham animals. Each bar represents the mean ± S.D. *$p < 0.05$ vs. Sham animals and #$p < 0.05$ vs. tGCI groups at the same time point. (**D**) Representative photomicrographs with fluorescent staining of mFKN (green) and NeuN (red) in CA1. Representative images show Sham group (a-c), 168 h after reperfusion of tGCI groups (d-f) and HPC groups (g-i), respectively. Scale bar, 25 μm

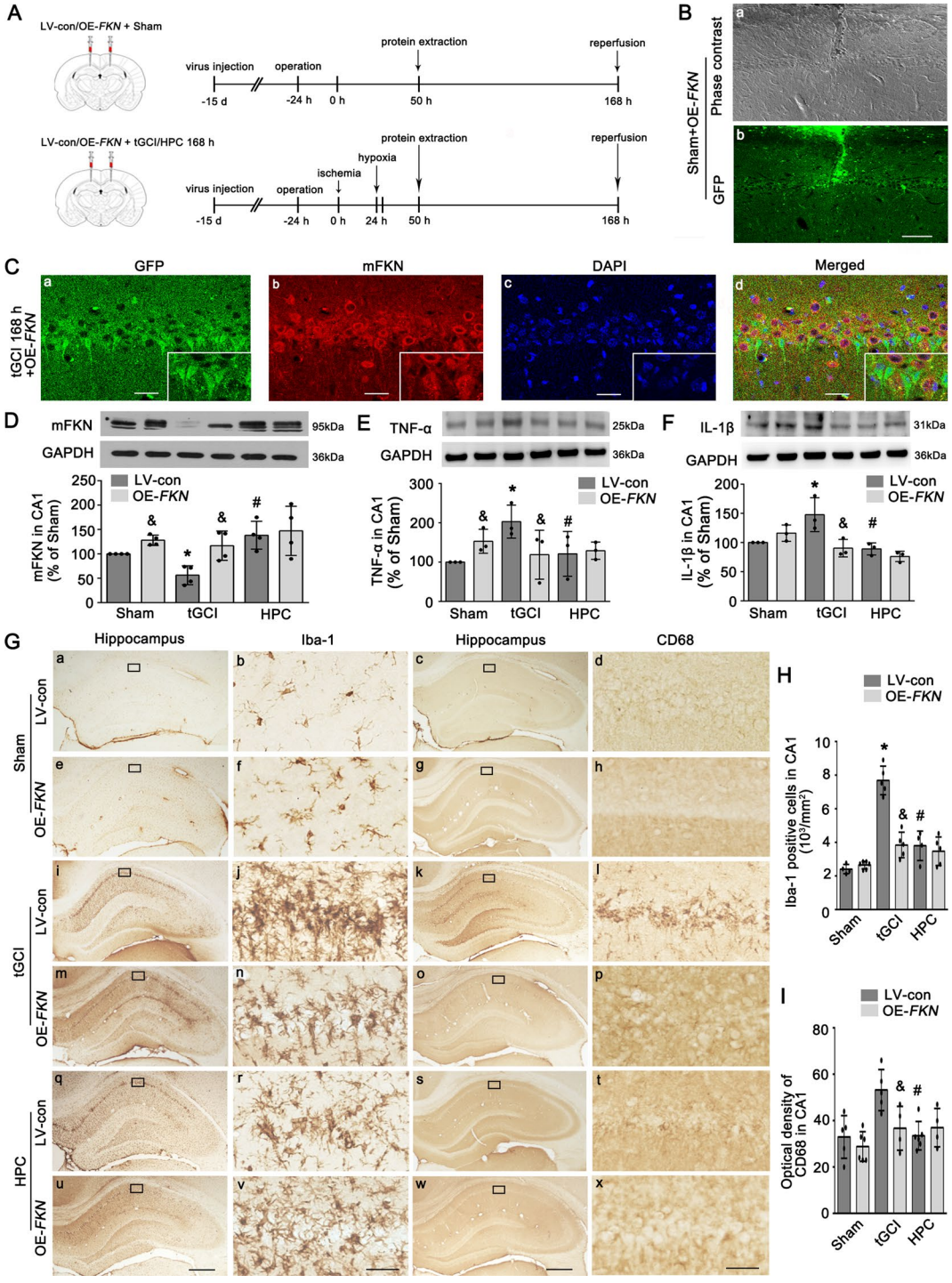

Fig. 3 The effects of FKN overexpression on inflammatory response and activation of microglia in CA1 after tGCI with or without HPC. (**A**) Design of experiments in which rats were stereotaxically injected with lentiviral vectors bilaterally into the dorsal CA1 pyramidal layer and subjected to either Sham or tGCI with hypoxia. (**B**) Phase contrast and fluorescent images from CA1 coronal sections of Sham group following with OE-*FKN* injection. Scale bar, 75 μm. (**C**) Representative photomicrographs show the co-localization of GFP (green), mFKN (red), and DAPI (blue) in CA1 from tGCI rats with OE-*FKN* injection. Scale bar, 25 μm. (**D**–**F**) Representative immunoblots showing the expressions of mFKN, TNF-α and IL-1β in CA1 with or without OE-*FKN* administration. The histogram presents the quantitative analyses of mFKN, TNF-α and IL-1β levels. Data are expressed as percentage of value of Sham animals. Each bar represents the mean ± S.D. (**G**) Representative microphotographs of Iba-1 and CD68 immunostaining in CA1 from rats administered bilaterally with either LV-con or OE-*FKN* at 168 h after reperfusion with or without hypoxia. Boxes indicate that the magnified regions displayed in the right panel. Scale bar, 250 μm (a, c, e, g, i, k, m, o, q, s, u, w) and 25 μm (b, d, f, h, j, l, n, p, r, t, v, x). (**H**, **I**) Quantitative analyses of Iba-1-positive cell and CD68-immunoreactivities in CA1. Each bar represents the mean ± S.D. **p* < 0.05 vs. Sham + LV-con animals, #*p* < 0.05 vs. tGCI group with LV-con, and &*p* < 0.05 vs. Sham/tGCI/HPC group with LV-con

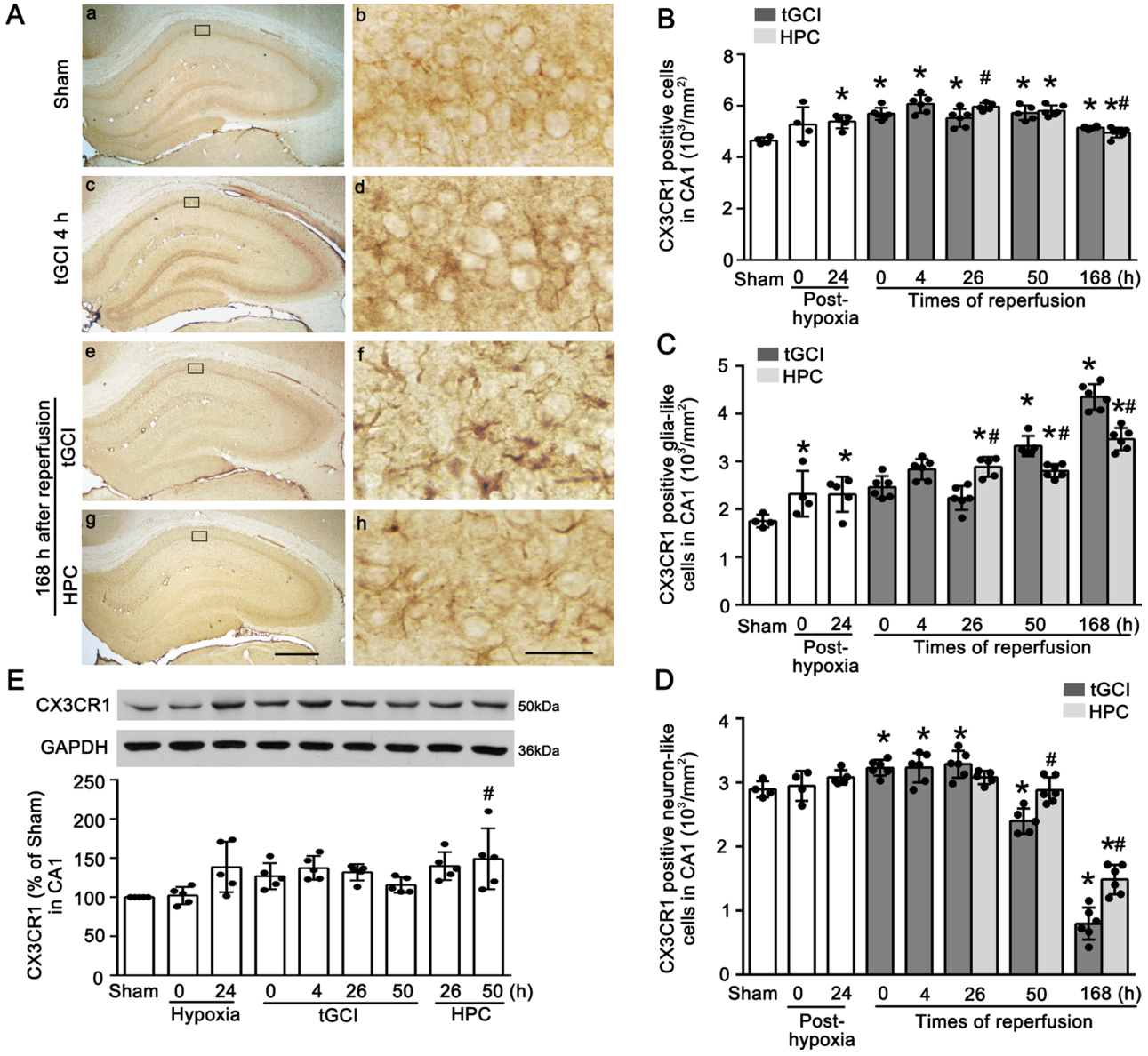

Fig. 4 The effects of HPC on the expression of CX3CR1 in CA1 after tGCI. (**A**) Immunohistochemistry of CX3CR1 in rat brains. Representative images show Sham group (a, b), 4 h after reperfusion of tGCI groups (c, d), 168 h after reperfusion of tGCI groups (e, f) and HPC groups (g, h), respectively. Scale bar, 250 μm (a, c, e, g) and 25 μm (b, d, f, h). (**B**) Quantitative analyses of CX3CR1-positive cells in CA1. (**C**) Quantitative analyses of CX3CR1-positive glia-like cells in CA1. (**D**) Quantitative analyses of CX3CR1-positive neuron-like cells in CA1. (**E**) Representative immunoblots showing the expression of CX3CR1 in CA1. The histogram presents the quantitative analyses of CX3CR1 levels. The horizontal axis of the chart represents times of reoxygenation or reperfusion. Data are expressed as percentage of value of Sham animals. Each bar represents the mean ± S.D. *$p < 0.05$ vs. Sham animals and #$p < 0.05$ vs. tGCI groups at the same time point

of CX3CR1-positive neuron-like cells at 50 h and 168 h after reperfusion (Fig. 4D). Western blotting analysis showed that CX3CR1 expression in CA1 increased at 50 h after reperfusion in HPC groups (Fig. 4E).

Examined by double-labeled immunofluorescence, CX3CR1 was mainly expressed in hippocampal neurons of Sham rats, as shown by the co-localization with NeuN, and low levels of CX3CR1 was expressed in astrocytes, as shown by the co-localization with GFAP (Fig. 5A). However, at 168 h after tGCI, CX3CR1-positive cells were mainly GFAP-positive, and only a few were colocalized with NeuN (Fig. 5B). Conversely, a majority of CX3CR1-positive cells in HPC rats exhibited similar appearance to neurons (Fig. 5C). Notably, only a few Iba-1-positive cells colocalized with CX3CR1-positive cells in CA1 of the rats described above. Quantitation showed that compared with Sham group, the expression of CX3CR1 in neurons of CA1 decreased after tGCI with or without hypoxia, and HPC repressed the reduction of CX3CR1 in neurons after tGCI. In contrast, the expression of

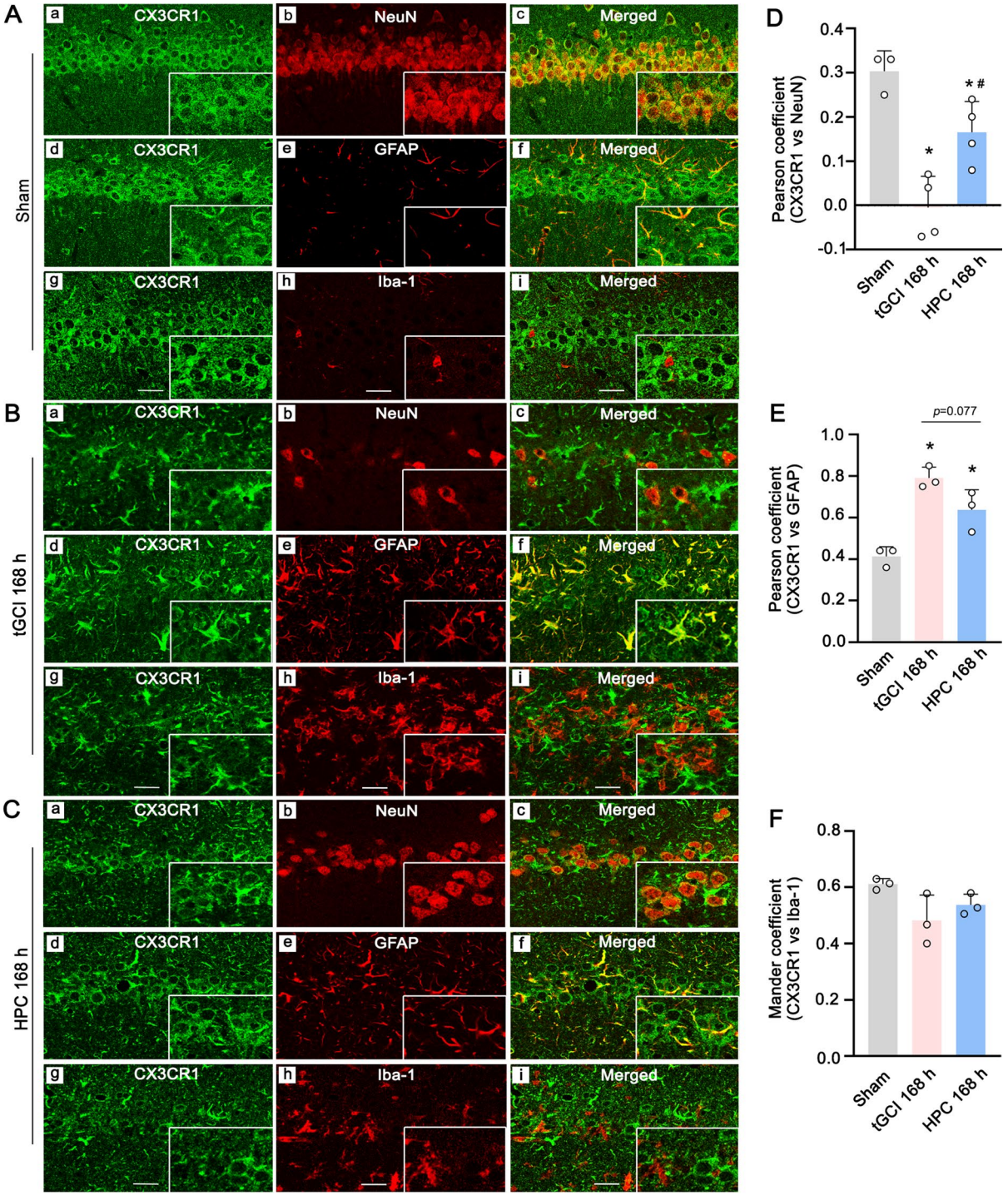

Fig. 5 The effects of HPC on the localization of CX3CR1 in CA1 after tGCI. (**A**) Representative photomicrographs with fluorescent staining of CX3CR1 (green) and NeuN/GFAP/Iba-1 (red) in CA1 of Sham group. (**B**) Representative photomicrographs with fluorescent staining of CX3CR1 (green) and NeuN/GFAP/Iba-1 (red) in CA1 of tGCI 168 h group. (**C**) Representative photomicrographs with fluorescent staining of CX3CR1 (green) and NeuN//GFAP/Iba-1 (red) in CA1 of HPC 168 h group. Rabbit derived CX3CR1 antibody was used for detecting the colocalization with NeuN and GFAP. Mouse derived CX3CR1 antibody was used for detecting the colocalization with Iba-1. Scale bar, 25 μm. (**D**) Quantification of colocalization CX3CR1 and NeuN with Pearson's coefficient in CA1. (**E**) Quantification of colocalization CX3CR1 and GFAP with Pearson's coefficient in CA1. (**F**) Quantification of colocalization CX3CR1 and Iba-1 with Mander's coefficient in CA1. Values represent the mean ± SD of three independent experiments. *$p < 0.05$ vs. Sham animals and #$p < 0.05$ vs. tGCI group

CX3CR1 in astrocytes increased after tGCI with or without hypoxia (Fig. 5D-F). The results above were reconfirmed by using another antibody of anti-rabbit CX3CR1 (Suppl Fig. S2). Additionally, in order to verify cell distribution of CX3CR1 at different time points of reperfusion, another antibody of anti-rabbit Iba-1 and anti-mouse CX3CR1 were used, the results of which established that a little bit of CX3CR1 is expressed in microglia at 0–50 h of reperfusion with or without hypoxia (Suppl Fig. S3). Furthermore, the expression of CX3CR1 mRNA was detected by FISH assay. As shown in Suppl Fig. S4, the mRNA of CX3CR1 was mainly expressed in neurons of Sham rats. However, at 168 h after tGCI, it was colocalized with GFAP and Iba-1.

The inhibitory experiments with lentivirus-mediated CX3CR1 knockdown were conducted to ascertain the role of CX3CR1 in the neuroprotection of HPC against tGCI. Rats were randomly subjected to Sham or tGCI at 14 days after the administration of CX3CRi-carried lentivirus (referred to as KD-*CX3CR1*) or scrambled lentivirus vector (referred to as LV-con) into the bilateral hippocampus. The efficacy of lentivirus transfection was hereby verified (Fig. 6A-C). As shown in Fig. 6B, the expression of CX3CR1 in glia-like cells decreased sharply at 168 h after reperfusion in CA1 of tGCI rats administrated with KD-*CX3CR1* compared with the rats administrated with LV-con. As expected, the administration of KD-*CX3CR1*, rather than LV-con, significantly reduced the CX3CR1 expression in Sham and tGCI rats (Fig. 6C). Meanwhile, KD-*CX3CR1* administration prevented the increase in the expression of TNF-α and IL-1β in CA1 after tGCI (Fig. 6D-E). However, KD-*CX3CR1* administration registered no significant effect on the expressions of TNF-α and IL-1β in CA1 after HPC. Accordingly, the effects of KD-*CX3CR1* administration on the microglial activation in CA1 after tGCI with or without hypoxia were examined (Fig. 6F-H), and the results showed that KD-*CX3CR1* administration reduced the number of Iba-1-positive cells in CA1 of tGCI rats. Also, rats injected with KD-*CX3CR1* in CA1 showed a significant decrease in the expression of CD68 compared with those rats injected with LV-con after tGCI. Nevertheless, either administration of KD-*CX3CR1* or LV-con had no significant effects on the number of Iba-1-positive cells and the expression of CD68 in CA1 after HPC. Afterwards, the effects of KD-*CX3CR1* administration on the neurons in CA1 after tGCI with or without hypoxia were tested (Fig. 6F, I-J), which showed that the administration of KD-*CX3CR1* or LV-con had no impact on the pyramidal neurons in CA1 of Sham rats, whereas KD-*CX3CR1* administration markedly ameliorated cellular damage and neuronal loss after tGCI.

The overexpression of FKN mediated by HPC increases neuronal CX3CR1 and p-Akt, reduced neuronal loss in CA1 after tGCI

As shown above, CX3CR1 can be expressed in neurons of CA1 after tGCI with or without hypoxia. Moreover, FKN directly modulates neuronal activity and survival *via* autoregulatory interaction [26]. Accordingly, we explored whether the neuronal FKN/CX3CR1 signal axis was involved in the neuroprotection induced by HPC after tGCI. As shown in Fig. 7A and B, OE-*FKN* administration increased the expression of CX3CR1 in neurons of CA1 at 168 h after tGCI. Western blotting analysis showed that CX3CR1 expression in CA1 was markedly increased in tGCI rats after OE-*FKN* administration (Fig. 7C). Furthermore, to verify the involvement of Akt signal pathway in the neuroprotection mediated by the neuronal FKN/CX3CR1 axis, we thus examined the levels of Akt and p-Akt (Ser473) in CA1 of rats after administration of OE-*FKN*. The results demonstrated that the administration of OE-*FKN* or LV-con had no impact on the expression of Akt either in Sham or tGCI rats with or without hypoxia (Fig. 7D). Nonetheless, compared with the administration of LV-con in tGCI rats, the phosphorylation of Akt (Ser473) was increased with OE-*FKN* (Fig. 7E). Accordingly, we examined the effects of OE-*FKN* administration on the neurons in CA1 after tGCI with or without hypoxia. As shown in Fig. 7F-H, the administration of OE-*FKN* showed no neurotoxic effect in CA1 of Sham rats, whereas, expectedly, the administration of OE-*FKN* significantly ameliorated cellular damage and neuronal lose at 168 h after tGCI.

Discussion

Accumulating evidence from clinical and animal studies indicates that ischemia-associated neuroinflammation within the brain is partially responsible for neuronal injury [38, 39]. In the present study, as shown in Fig. 8 (drawing by Figdraw (www.figdraw.com)), we report that tGCI stimulated microglial activation and neuroinflammation through activation of CX3CR1 in astrocytes, resulting in neuronal damage in hippocampal CA1 of rats. We also found that HPC upregulated endogenous FKN expressed in neurons and limited the activation of CX3CR1 on glial cells, thereby inhibiting microglial neuroinflammation in CA1 after tGCI. Meanwhile, the overexpression of FKN mediated by HPC increased CX3CR1 in neurons and upregulated p-Akt which were probably involved in reduced neuronal loss after tGCI (Fig. 8). According to this study, HPC protected against neuronal damage in CA1 after tGCI, perhaps through inhibiting microglial neuroinflammation and activating Akt, which was mediated by FKN/CX3CR1 axis in the neuronal network.

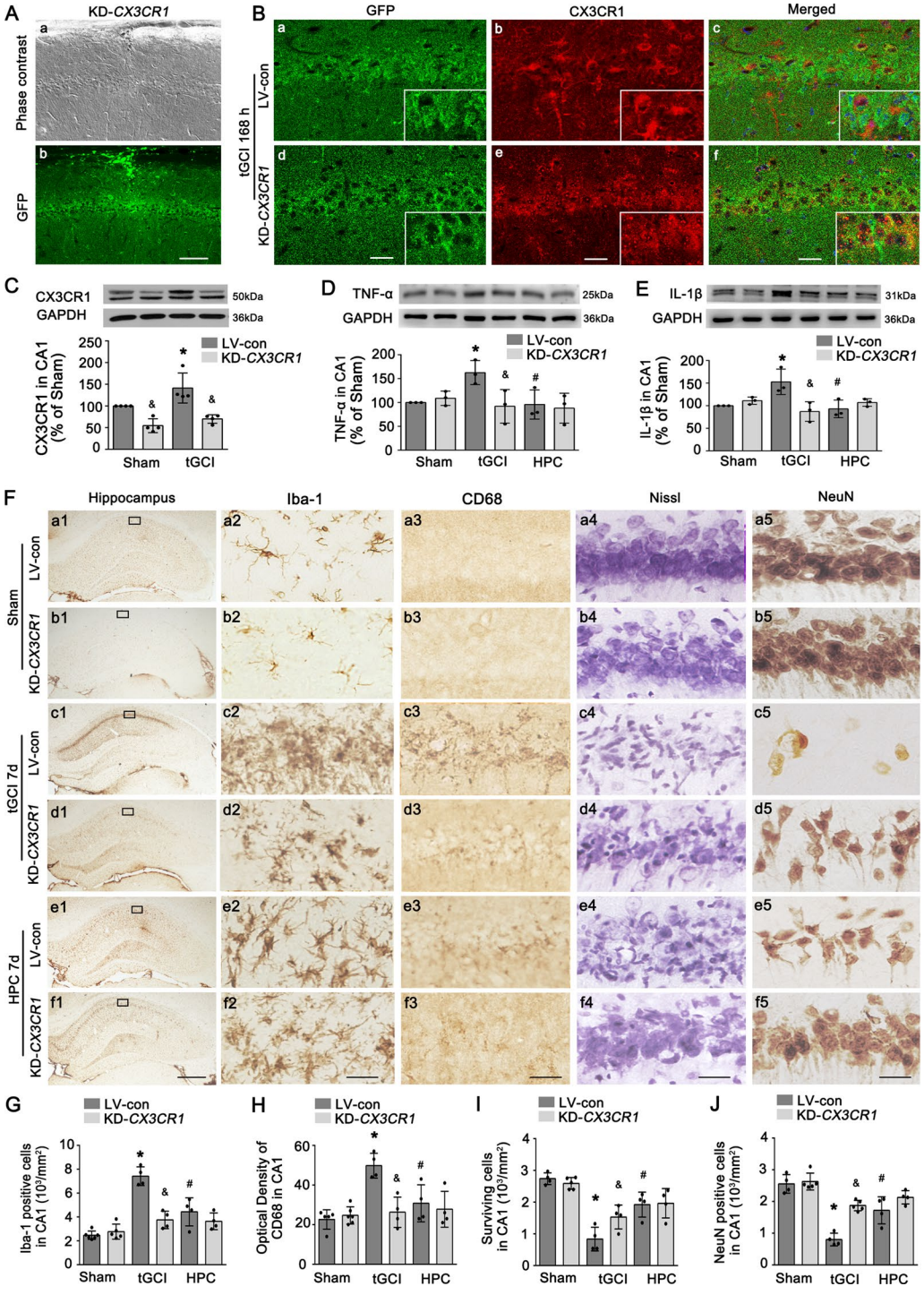

Fig. 6 The effects of CX3CR1 knockdown on the neuronal damage and inflammatory response in CA1 after tGCI with or without HPC. (**A**) Phase contrast and fluorescent images from CA1 coronal sections of Sham group with KD-*CX3CR1*. Scale bar, 75 μm. (**B**) Representative photomicrographs show the co-localization of GFP (green) and CX3CR1 (red) in CA1 from 168 h after reperfusion of tGCI groups with LV-con or KD-*CX3CR1* injection. Scale bar, 25 μm. (**C**–**E**) Representative immunoblots showing the expressions of CX3CR1, TNF-α and IL-1β in CA1 with or without KD-*CX3CR1* administration. The histogram presents the quantitative analyses of CX3CR1, TNF-α and IL-1β levels. Data are expressed as percentage of value of Sham animals. Each bar represents the mean ± S.D. (**F**) Representative microphotographs of Iba-1 and CD68 immunostaining, cresyl violet staining and NeuN immunostaining in CA1 from rats administered bilaterally with either LV-con or KD-*CX3CR1* at 168 h after reperfusion with or without hypoxia. Boxes indicate that the magnified regions displayed in the right panel. Scale bar, 250 μm (a1-f1) and 25 μm (a2-f2, a3-f3, a4-f4). (**G**–**J**) Quantitative analyses of Iba-1-positive cell, CD68-immunoreactivities, surviving cells and NeuN-positive cells in CA1. Each bar represents the mean ± S.D. *$p < 0.05$ vs. Sham + LV-con animals, # $p < 0.05$ vs. tGCI group with LV-con, and & $p < 0.05$ vs. Sham/tGCI/HPC group with LV-con

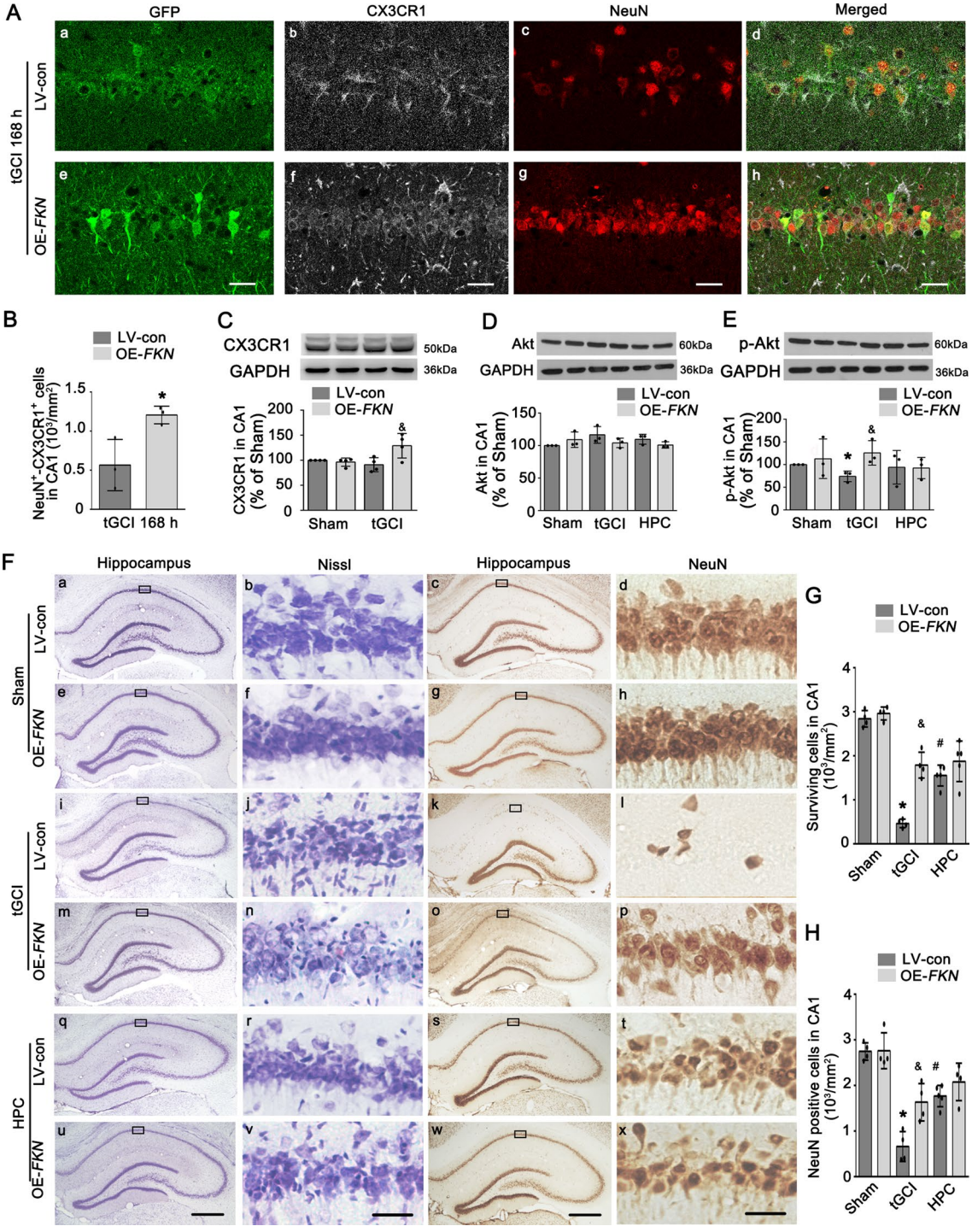

Fig. 7 The effects of FKN overexpression on the neuronal damage and the expression of CX3CR1 and p-Akt in CA1 after tGCI with or without HPC. (**A**) Representative photomicrographs show the co-localization of GFP (green), CX3CR1 (gray) and NeuN (red) in CA1 from 168 h after reperfusion of tGCI groups with LV-con or OE-*FKN* injection. Scale bar, 25 μm. (**B**) Quantitative analyses of CX3CR1-positive cell in neurons of CA1 from 168 h after reperfusion of tGCI groups with LV-con or OE-*FKN* injection. (**C**–**E**) Representative immunoblots showing the expressions of CX3CR1, Akt and p-Akt in CA1 with or without OE-*FKN* administration. The histogram presents the quantitative analyses of CX3CR1, Akt and p-Akt levels. Data are expressed as percentage of value of Sham animals. Each bar represents the mean ± S.D. (**F**) Representative microphotographs of cresyl violet staining and NeuN immunostaining in CA1 from rats administered bilaterally with either LV-con or OE-*FKN* at 168 h after reperfusion with or without hypoxia. Boxes indicate that the magnified regions displayed in the right panel. Scale bar, 250 μm (a, c, e, g, i, k, m, o, q, s, u, w) and 25 μm (b, d, f, h, j, l, n, p, r, t, v, x). (**G**, **J**) Quantitative analyses of surviving cells and NeuN-positive cells in CA1. Each bar represents the mean ± S.D. *$p < 0.05$ vs. Sham + LV-con animals, #$p < 0.05$ vs. tGCI group with LV-con, and &$p < 0.05$ vs. Sham/tGCI/HPC group with LV-con

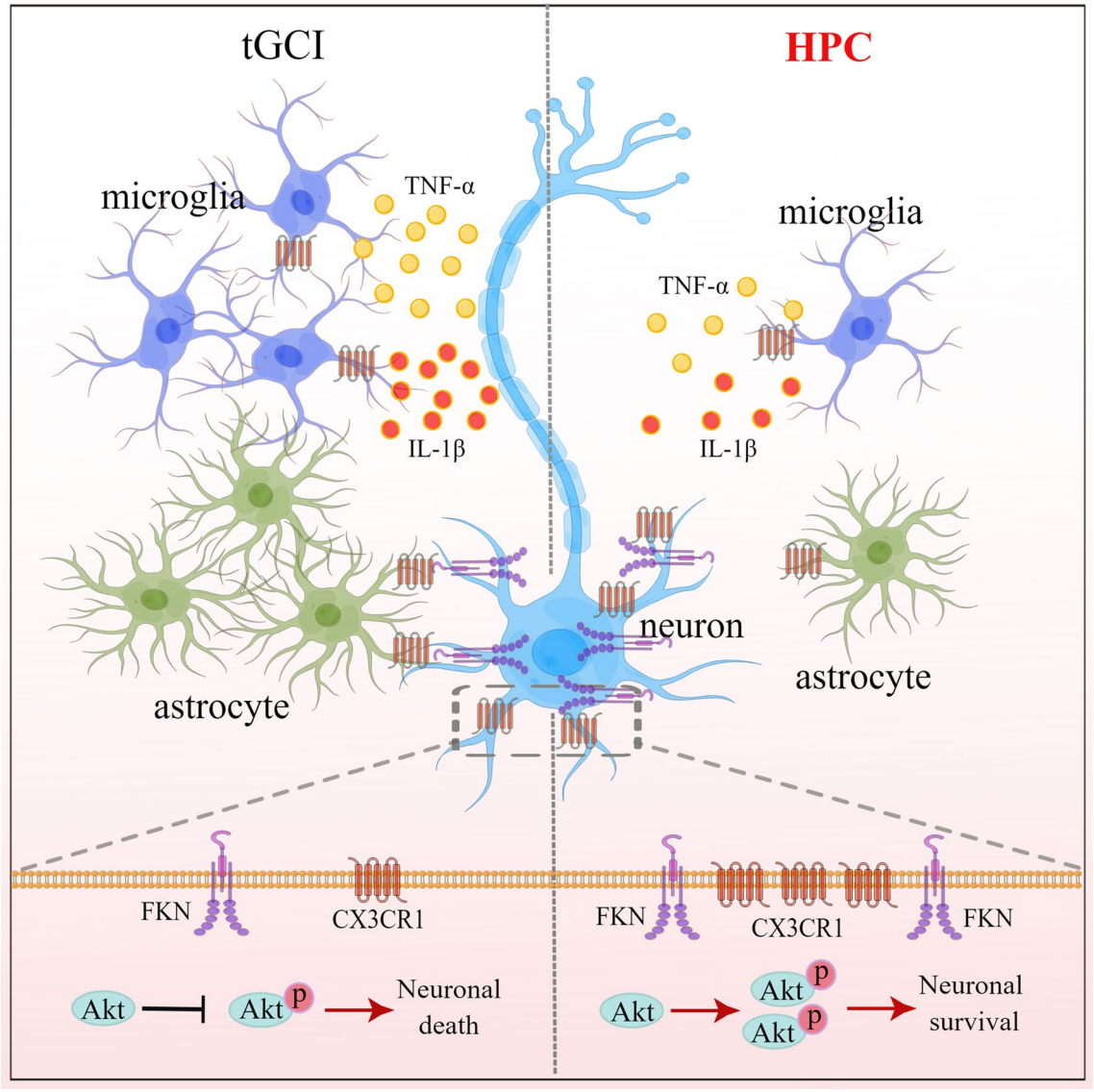

Fig. 8 Schematic depicting mechanism by which HPC protects neuron against tGCI in the hippocampal CA1 through regulating FKN/CX3CR1 axis. HPC activates the FKN/CX3CR1 axis in neurons, and then upregulates the phosphorylation of Akt, thereby protecting neurons in CA1 against tGCI. Meanwhile, HPC downregulates the expression of CX3CR1 in glial cells, thereby preventing the excessive activation of microglia and inhibiting the production of proinflammatory cytokines in CA1 after tGCI

Microglia/macrophages, the first line of defense against CNS injuries, exert a crucial effect on maintaining brain homeostasis. The resident mocroglia and peripheral macrophage are rapidly activated after cerebral ischemia [40], and they play a pivotal part in regulating neuroinflammation, implicated in the pathological process of ischemic brain injury. Cerebral ischemia not only induces neuronal death but also promotes activation of microglia. Dying neurons release neurotoxic factors that promote activation of microglia, resulting in excessive release of proinflammatory cytokines, which in turn triggers an inflammatory response and aggravates neuronal damage after cerebral ischemia [41]. In opposition, inhibiting the activation of microglia and reducing the release of inflammatory mediators would alleviate neuronal damage, reduce infarct volume and improve neurological function [42, 43]. In this study, we found that the number of Iba-1 immunopositive cells increased and the expression of the activating marker CD68 in CA1 enhanced at 168 h after tGCI. Meanwhile, the expression of proinflammatory cytokine was found to be upregulated. Nonetheless, microglia in CA1 of HPC rats displayed a more resting morphology, and the expression of CD68 and proinflammatory cytokines decreased. These results imply that HPC inhibits the activation of microglia and the release of proinflammatory cytokines in CA1 after tGCI.

In the CNS, the interaction between neurons and glial cells is an important endogenous mechanism for neurons to inhibit excessive activation of microglia, in which FKN/CX3CR1 axis plays a crucial role [44]. Under physiological conditions, neuron-derived FKN suppresses microglial activation and maintains them in a resting state through binding to its receptor CX3CR1 on microglia [45]. However, during pathological states, the expression of FKN was reduced, resulting in attenuation of the FKN-CX3CR1 interactions between neurons and microglia, and consequently activating the microglia-induced inflammation. For example, Lyons et al. [46] have shown that in aged rats, the levels of FKN in the hippocampus were downregulated, which was correlated with an increase in CX3CR1 expression and microglial activation. Moreover, FKN has also been shown to inhibit the lipopolysaccharide-induced microglial activation and reduce the release of inflammatory, such as TNF-α [47]. Interestingly, the expression of FKN in neurons of ischemic penumbra was decreased following focal cerebral ischemia-reperfusion, accompanied by the activation of microglia and the secretion of proinflammatory cytokines, such as TNF-α and IL-1β [48]. In addition, the intracerebroventricular administration of exogenous FKN resulted in a long-lasting neuroprotective effect on cerebral ischemia in rodents [49, 50]. Similarly, our study demonstrated a reduction of mFKN expression in CA1 after tGCI, whereas this trend was reversed by HPC. Furthermore, the overexpression of FKN in CA1 mediated by FKN-carried lentivirus would inhibit microglial activation and attenuate the release of inflammatory factors after tGCI, which was similar to the effects of HPC. These data suggest that a high level of endogenous or exogenous FKN expressed in neurons limits CX3CR1 activation on glial cells, and thus keeping microglia in a quiescent state. HPC suppresses microglial activation with neuroinflammation in hippocampal CA1 induced by tGCI via upregulating the expression of FKN.

In general, FKN exists in two forms, mFKN and sFKN. In the peripheral immune system, mFKN is adhesive and mediates the adhesion of leukocytes to the surface of endothelial cells. Whereas, sFKN, with chemotaxis, induces the expression of cell surface binding proteins on the surface of activated primary endothelial cells to promote strong adhesion of white blood cells [10–13]. However, the roles of mFKN and sFKN in the activation of microglia in CNS remain to be elucidated. In a mouse model of Parkinson's disease, the overexpression of sFKN by the administration of sFKN-carried adeno-associated virus in substantia nigra neurons would ameliorate microglia activation and proinflammatory factors release, then alleviate the loss of substantia nigra neurons, and thus exerting neuroprotective effects; yet mFKN has no similar effects [15]. However, in a transgenic mouse models of Alzheimer's disease, it is mFKN, but not sFKN, which regulates microglial phagocytosis of Aβ and neuronal microtubule-associated protein tau phosphorylation [51]. The current study has expanded these findings to examine the roles of mFKN and sFKN in microglial activation after cerebral ischemia. We found that tGCI reduced the expression of mFKN in CA1, and HPC prevented this reduction after tGCI. On the other hand, the expression of sFKN in CA1 increased after tGCI, while HPC had no significant effect on its expression. Therefore, this important finding may provide evidence that mFKN, rather than sFKN, could be involved in a potential mechanism for attenuating neuroinflammation induced by HPC against tGCI.

In contrast to the exclusive location in neurons of FKN, the expression of CX3CR1 in the CNS is still somewhat controversial [8]. Ahn et al. found that the expression of CX3CR1 in CA1 pyramidal neurons was significantly increased at 1 day after 5 min of bilateral carotid artery occlusion in gerbils, and it gradually decreased thereafter. Nevertheless, the expression of CX3CR1 was markedly increased in microglia after 5 days of reperfusion [52]. Wang et al. observed in permanent MCAO model, elevated neuronal CX3CR1 expression in the peri-infarct, hippocampus and striatum after ischemia [53]. Contrary to these finding, other studies suggested CX3CR1 expresses restrictively in microglia [54–56]. In this study, we demonstrate that CX3CR1, including CX3CR1 protein and mRNA, was mainly expressed in neurons in CA1 of Sham rats. Interestingly, CX3CR1, present in astrocytes, gradually increased post-tGCI, while HPC reduced its expression in astrocytes. What is noteworthy is that a shade of CX3CR1 was expressed in microglia in CA1. There have been reported that CX3CR1 was expressed in astrocytes of brain samples including human and rodent, both in vivo and in vitro [57, 58]. The localization of CX3CR1 in astrocytes implicates that FKN/CX3CR1 axis may play a role in modulating astrocyte reactivity. Additionally, it is possible that astrocyte-derived CX3CR1 induce the release of soluble mediators to promote microglial proliferation [27], which may involve in the communication between astrocytes and microglia. For example, after cerebral ischemic injury in mice, activated astrocytes in the brain tissue can secrete IL-15 and other inflammatory mediators, thus aggravating neuronal damage [59]. In addition, in the ischemic penumbra of human brain tissue, astrocytes can activate microglia, which in turn triggers an inflammatory response and aggravates neuronal damage [60]. Although these mediators remain to be identified, the different cellular distributions of FKN and CX3CR1 in CA1 of Sham and operated rats in our study suggest that FKN/CX3CR1 axis are involved in more complex signaling among neurons, astrocytes and

microglia in the pathophysiology of cerebral ischemia, rather than just mediating neuron-microglia crosstalk.

In order to ascertain the role of CX3CR1 in the neuroprotection of HPC against tGCI, the inhibitory experiments with lentivirus-mediated CX3CR1 knockdown were conducted. The results showed that inhibiting the expression of CX3CR1 reduced the activation of microglia in CA1 after tGCI and promoted neuronal survival. Similarly, research by Tang et al. found that knocking out *CX3CR1* in adult male mice causes a significant reduction in microglial activation and inflammatory mediator release, thus alleviating neurological deficits after MCAO [61]. Intriguingly, although CX3CR1 expresses in both neurons and glial cells in CA1, administrated with KD-*CX3CR1* in tGCI rats decreased sharply the expression of CX3CR1 in glia-like cells. In this study, using LV-*CX3CR1*-RNAi, we observed that inhibiting the expression of CX3CR1 in glial cells reduced the activation of microglia in CA1 after tGCI and promoted neuronal survival. Therefore, it seems logical to state that the activation of CX3CR1 in glial cells after cerebral ischemia led to microglial activation and aggravates neuronal damage. Further investigation, such as using lentivirus-delivered particles with specific promoter or in vitro experiment, will be required to elucidate the roles of CX3CR1 in different cells. In addition, though the overexpression of FKN or silencing of CX3CR1 was mimicking the effect of HPC, the loss of function verification should be more important.

As stated above, FKN reduces microglial activation, and inhibits inflammatory cytokines, thereby contributing to its neuroprotective effects. Indeed, given the fact that FKN is mainly expressed in neurons, it is imperative to investigate the direct effects of FKN on neurons. Heinisch and Kirby reported that FKN inhibits the raphe serotonin neurons by enhancing the activity of GABAergic receptors. Interestingly, over 70% of these neurons exhibits FKN/CX3CR1 co-localization [62]. In fact, in our study, most CX3CR1-positive cells in CA1 of Sham and HPC rats were neurons. Specifically, the overexpression of FKN in CA1 led to a significant increase in the expression of CX3CR1 in neurons, further suggesting that FKN exerted a direct neuroprotective effect on neurons, as opposed to indirect actions through microglia-mediated neuromodulation. Based on this noteworthy discovery, it is crucial to elucidate the mechanisms of FKN-mediated neuroprotective effect *via* autoregulatory interaction. Several studies in vitro cell culture systems have investigated the role of the FKN-mediated intracellular signaling in neurons. For example, Deiva et al. reported that the treatment of human neurons with FKN induced phosphorylation of extracellular signal-regulated kinase 1/2 (ERK1/2) and Akt after exposed to glutamate receptor-mediated excitotoxicity [63]. In addition, FKN inhibits glutamate receptor-mediated neuron apoptosis, but this neuroprotective effect is abolished by blocking Akt and ERK1/2 signaling pathway [63]. It was further confirmed by Limatola et al. that neurons-derived FKN activates Akt through acting on CX3CR1 in neurons, and reduces neuronal apoptosis induced by glutamate [29]. FKN also rapidly increased Akt activation in microglia in a dose- and time-dependent manner [27]. However, to our best knowledge, there has been no study in vivo to explore the effects of FKN/CX3CR1 axis on Akt signaling pathway so far. Our in vivo results demonstrate that the overexpression of FKN induces a significant increase in phospho-Akt levels which correlated with marked neuroprotection of hippocampal neurons in CA1 after tGCI. Moreover, our previous study found that phospho-Akt is exclusively located in neurons of CA1 with or without tGCI [34]. Unfortunately, we did not investigate the effect of Akt suppressor and inducer after overexpression of FKN on the neuroprotection of HPC against tGCI, including neurological functional tests. In addition, further investigation, such as the knockdown of neuronal CX3CR1 in CA1 after overexpression of FKN, will be required to elucidate the roles of neuronal FKN/CX3CR1 axis in the activation of Akt signaling pathways. Nonetheless, these works give credence to the hypothesis that FKN can increase neuronal CX3CR1, activate Akt signaling pathway and mediate HPC-induced neuroprotection against tGCI.

In this study, we have provided evidence for a potential mechanism of HPC-induced anti-inflammation and neuroprotection against tGCI through driving the FKN/CX3CR1 axis in CA1. The FKN/CX3CR1 axis seems to have evolved as a communication link between neurons and glial cells after cerebral ischemia. Moreover, our study established that FKN, rather than merely a chemotactic factor, may mediate neuroprotective effects on cerebral ischemia *via* activation of Akt signal pathway. Thus, FKN/CX3CR1 axis may be an attractive potential therapeutic target for anti-inflammation and neuroprotection after cerebral ischemia.

Abbreviations

FKN	Fractalkine
CX3CR1	CX3C chemokine receptor 1
HPC	Hypoxic postconditioning
tGCI	Transient global cerebral ischemia
CA1	Cornu amonis 1
CNS	Central nervous system
TNF	Tumor necrosis factor
IL	Interleukin
CD	Cluster of differentiation
mFKN	Membrane-anchored FKN
sFKN	Soluble FKN
Sham	Sham-operated
Iba-1	Ionized calcium binding adaptor molecule-1
GFAP	Glial fibrillary acidic protein

Supplementary Information

The online version contains supplementary material available at https://doi.org/10.1186/s12964-024-01830-4.

Supplementary Material 1

Supplementary Material 2

Acknowledgements
Our sincere thanks go to Peifeng Du (Guangzhou International Bio Island Co., Ltd) for editing this paper. The schematic figure was drawn by Figdraw (www.figdraw.com).

Author contributions
EX and LZ conceived the study, designed and assembled all figures. MQ, JZ, ML, KL performed the experiments with the help of WS and JD. MQ and JZ performed data analysis. MQ prepared the figures with the help of LZ and WS. EX, LZ and MQ wrote the manuscript. All authors read and approved the final manuscript.

Funding
This work was supported by the Natural Science Foundation of Guangdong Province, China (No. 2021A1515011269), the National Natural Science Foundation of China (No. 82271330; 82071281) and Key Medical Disciplines and Specialties Program of Guangzhou (2021–2023).

Data availability
No datasets were generated or analysed during the current study.

Declarations

Ethics approval and consent to participate
Not applicable for humans since there are no human subjects or samples in this study. All surgical procedures and animal experiments were performed according to the Animal Research: Reporting In Vivo Experiments guidelines and were approved and monitored by the Animal Care and Use Committee of Guangzhou Medical University.

Consent for publication
This manuscript has been approved for publication by all authors.

Competing interests
The authors declare no competing interests.

Received: 29 April 2024 / Accepted: 15 September 2024
Published online: 26 September 2024

References

1. Kirino T. Delayed neuronal death in the gerbil hippocampus following ischemia. Brain Res. 1982;23(1):57–69.
2. Lu X, Zhan L, Chai G, Chen M, Sun W, Xu E. Hypoxic preconditioning attenuates Neuroinflammation via inhibiting NF-κB/NLRP3 Axis mediated by p-MLKL after transient global cerebral ischemia. Mol Neurobiol. 2024;61(2):1080–99.
3. Yew WP, Djukic ND, Jayaseelan JSP, Woodman RJ, Muyderman H, Sims NR. Differential effects of the cell cycle inhibitor, olomoucine, on functional recovery and on responses of peri-infarct microglia and astrocytes following photothrombotic stroke in rats. J Neuroinflammation. 2021;18(1):168.
4. Mao M, Xu Y, Zhang XY, Yang L, An XB, Qu Y, et al. MicroRNA-195 prevents hippocampal microglial/macrophage polarization towards the M1 phenotype induced by chronic brain hypoperfusion through regulating CX3CL1/CX3CR1 signaling. J Neuroinflammation. 2020;17(1):244.
5. Lu Y, Zhou M, Li Y, Li Y, Hua Y, Fan Y. Minocycline promotes functional recovery in ischemic stroke by modulating microglia polarization through STAT1/STAT6 pathways. Biochem Pharmacol. 2021;186:114464.
6. Mota M, Porrini V, Parrella E, Benarese M, Bellucci A, Rhein S, et al. Neuroprotective epi-drugs quench the inflammatory response and microglial/macrophage activation in a mouse model of permanent brain ischemia. J Neuroinflammation. 2020;17(1):361.
7. Zhan L, Li D, Liang D, Wu B, Zhu P, Wang Y, et al. Activation of Akt/FoxO and inactivation of MEK/ERK pathways contribute to induction of neuroprotection against transient global cerebral ischemia by delayed hypoxic postconditioning in adult rats. Neuropharmacology. 2012;63(5):873–82.
8. Subbarayan MS, Joly-Amado A, Bickford PC, Nash KR. CX3CL1/CX3CR1 signaling targets for the treatment of neurodegenerative diseases. Pharmacol Ther. 2022;231:107989.
9. You M, Long C, Wan Y, Guo H, Shen J, Li M, et al. Neuron derived fractalkine promotes microglia to absorb hematoma via CD163/HO-1 after intracerebral hemorrhage. Cell Mol Life Sci. 2022;79(5):224.
10. Bazan JF, Bacon KB, Hardiman G, Wang W, Soo K, Rossi D, et al. A new class of membrane-bound chemokine with a CX3C motif. Nature. 1997;385(6617):640–4.
11. Fong AM, Erickson HP, Zachariah JP, Poon S, Schamberg NJ, Imai T, et al. Ultrastructure and function of the fractalkine mucin domain in CX(3)C chemokine domain presentation. J Biol Chem. 2000;275(6):3781–6.
12. Hermand P, Pincet F, Carvalho S, Ansanay H, Trinquet E, Daoudi M, et al. Functional adhesiveness of the CX3CL1 chemokine requires its aggregation. Role of the transmembrane domain. J Biol Chem. 2008;283(44):30225–34.
13. Pan Y, Lloyd C, Zhou H, Dolich S, Deeds J, Gonzalo JA, et al. Neurotactin, a membrane-anchored chemokine upregulated in brain inflammation. Nature. 1997;387(6633):611–7.
14. Liu C, Hong K, Chen H, Niu Y, Duan W, Liu Y, et al. Evidence for a protective role of the CX3CL1/CX3CR1 axis in a model of amyotrophic lateral sclerosis. Biol Chem. 2019;400(5):651–61.
15. Morganti JM, Nash KR, Grimmig BA, Ranjit S, Small B, Bickford PC, et al. The soluble isoform of CX3CL1 is necessary for neuroprotection in a mouse model of Parkinson's disease. J Neurosci. 2012;32(42):14592–601.
16. Pabon MM, Bachstetter AD, Hudson CE, Gemma C, Bickford PC. CX3CL1 reduces neurotoxicity and microglial activation in a rat model of Parkinson's disease. J Neuroinflammation. 2011;8:9.
17. Nash KR, Moran P, Finneran DJ, Hudson C, Robinson J, Morgan D, et al. Fractalkine over expression suppresses α-synuclein-mediated neurodegeneration. Mol Ther. 2015;23(1):17–23.
18. Ridderstad Wollberg A, Ericsson-Dahlstrand A, Juréus A, Ekerot P, Simon S, Nilsson M, et al. Pharmacological inhibition of the chemokine receptor CX3CR1 attenuates disease in a chronic-relapsing rat model for multiple sclerosis. Proc Natl Acad Sci U S A. 2014;111(14):5409–14.
19. Lee S, Varvel NH, Konerth ME, Xu G, Cardona AE, Ransohoff RM, et al. CX3CR1 deficiency alters microglial activation and reduces beta-amyloid deposition in two Alzheimer's disease mouse models. Am J Pathol. 2010;177(5):2549–62.
20. Puntambekar SS, Moutinho M, Lin PB, Jadhav V, Tumbleson-Brink D, Balaji A, et al. CX3CR1 deficiency aggravates amyloid driven neuronal pathology and cognitive decline in Alzheimer's disease. Mol Neurodegener. 2022;17(1):47.
21. Wang X, Xie Y, Niu Y, Wan B, Lu Y, Luo Q, et al. CX3CL1/CX3CR1 signal mediates M1-type microglia and accelerates high-altitude-induced forgetting. Front Cell Neurosci. 2023;17:1189348.
22. Harrison JK, Jiang Y, Chen S, Xia Y, Maciejewski D, McNamara RK, et al. Role for neuronally derived fractalkine in mediating interactions between neurons and CX3CR1-expressing microglia. Proc Natl Acad Sci U S A. 1998;95(18):10896–901.
23. Bajetto A, Bonavia R, Barbero S, Schettini G. Characterization of chemokines and their receptors in the central nervous system: physiopathological implications. J Neurochem. 2002;82(6):1311–29.
24. Lee M, Lee Y, Song J, Lee J, Chang SY. Tissue-specific role of CX3CR1 expressing immune cells and their relationships with human disease. Immune Netw. 2018;18(1):e5.
25. Dorf ME, Berman MA, Tanabe S, Heesen M, Luo Y. Astrocytes express functional chemokine receptors. J Neuroimmunol. 2000;111(1–2):109–21.
26. Jiang Y, Salafranca MN, Adhikari S, Xia Y, Feng L, Sonntag MK, et al. Chemokine receptor expression in cultured glia and rat experimental allergic encephalomyelitis. J Neuroimmunol. 1998;86(1):1–12.
27. Maciejewski-Lenoir D, Chen S, Feng L, Maki R, Bacon KB. Characterization of fractalkine in rat brain cells: migratory and activation signals for CX3CR-1-expressing microglia. J Immunol. 1999;163(3):1628–35.
28. Meucci O, Fatatis A, Simen AA, Miller RJ. Expression of CX3CR1 chemokine receptors on neurons and their role in neuronal survival. Proc Natl Acad Sci U S A. 2000;97(14):8075–80.

29. Limatola C, Lauro C, Catalano M, Ciotti MT, Bertollini C, Di Angelantonio S, et al. Chemokine CX3CL1 protects rat hippocampal neurons against glutamate-mediated excitotoxicity. J Neuroimmunol. 2005;166(1–2):19–28.
30. Yano S, Morioka M, Fukunaga K, Kawano T, Hara T, Kai Y, et al. Activation of Akt/protein kinase B contributes to induction of ischemic tolerance in the CA1 subfield of gerbil hippocampus. J Cereb Blood Flow Metab. 2001;21(4):351–60.
31. Kitano H, Young JM, Cheng J, Wang L, Hurn PD, Murphy SJ. Gender-specific response to isoflurane preconditioning in focal cerebral ischemia. J Cereb Blood Flow Metab. 2007;27(7):1377–86.
32. Pulsinelli W, Brierley J. A new model of bilateral hemispheric ischemia in the unanesthetized rat. Stroke. 1979;10(3):267–72.
33. Zhan L, Lu X, Xu W, Sun W, Xu E. Inhibition of MLKL-dependent necroptosis via downregulating interleukin-1R1 contributes to neuroprotection of hypoxic preconditioning in transient global cerebral ischemic rats. J Neuroinflammation. 2021;18(1):97.
34. Zhan L, Wang T, Li W, Xu ZC, Sun W, Xu E. Activation of Akt/FoxO signaling pathway contributes to induction of neuroprotection against transient global cerebral ischemia by hypoxic pre-conditioning in adult rats. J Neurochem. 2010;114(3):897–908.
35. Wang Y, Zhan L, Zeng W, Li K, Sun W, Xu Z, et al. Downregulation of hippocampal GABA after hypoxia-induced seizures in neonatal rats. Neurochem Res. 2011;36(12):2409–16.
36. Hase Y, Ameen-Ali KE, Waller R, Simpson JE, Stafford C, Mahesh A, et al. Differential perivascular microglial activation in the deep white matter in vascular dementia developed post-stroke. Brain Pathol. 2022;32(6):e13101.
37. Karperien A, Ahammer H, Jelinek HF. Quantitating the subtleties of microglial morphology with fractal analysis. Front Cell Neurosci. 2013;7:3.
38. Candelario-Jalil E, Dijkhuizen RM, Magnus T. Neuroinflammation, stroke, blood-brain barrier dysfunction, and imaging modalities. Stroke. 2022;53(5):1473–86.
39. Qiu M, Xu E, Zhan L. Epigenetic regulations of microglia/macrophage polarization in ischemic stroke. Front Mol Neurosci. 2021;14:697416.
40. Kanazawa M, Ninomiya I, Hatakeyama M, Takahashi T, Shimohata T. Microglia and monocytes/macrophages polarization reveal novel therapeutic mechanism against stroke. Int J Mol Sci. 2017;18(10):2135.
41. Zhao SC, Ma LS, Chu ZH, Xu H, Wu WQ, Liu F. Regulation of microglial activation in stroke. Acta Pharmacol Sin. 2017;38(4):445–58.
42. Yang C, Gong S, Chen X, Wang M, Zhang L, Zhang L, et al. Analgecine regulates microglia polarization in ischemic stroke by inhibiting NF-κB through the TLR4 MyD88 pathway. Int Immunopharmacol. 2021;99:107930.
43. Rahimian R, Lively S, Abdelhamid E, Lalancette-Hebert M, Schlichter L, Sato S, et al. Delayed galectin-3-mediated reprogramming of microglia after stroke is protective. Mol Neurobiol. 2019;56(9):6371–85.
44. Pawelec P, Ziemka-Nalecz M, Sypecka J, Zalewska T. The Impact of the CX3CL1/CX3CR1 Axis in Neurological Disorders. Cells. 2020;9(10):2277.
45. Ludwig A, Weber C. Transmembrane chemokines: versatile 'special agents' in vascular inflammation. Thromb Haemost. 2007;97(5):694–703.
46. Lyons A, Lynch AM, Downer EJ, Hanley R, O'Sullivan JB, Smith A, et al. Fractalkine-induced activation of the phosphatidylinositol-3 kinase pathway attentuates microglial activation in vivo and in vitro. J Neurochem. 2009;110(5):1547–56.
47. Zujovic V, Benavides J, Vigé X, Carter C, Taupin V. Fractalkine modulates TNF-alpha secretion and neurotoxicity induced by microglial activation. Glia. 2000;29(4):305–15.
48. He HY, Ren L, Guo T, Deng YH. Neuronal autophagy aggravates microglial inflammatory injury by downregulating CX3CL1/fractalkine after ischemic stroke. Neural Regen Res. 2019;14(2):280–8.
49. Qin W, Li Z, Luo S, Wu R, Pei Z, Huang R. Exogenous fractalkine enhances proliferation of endothelial cells, promotes migration of endothelial progenitor cells and improves neurological deficits in a rat model of ischemic stroke. Neurosci Lett. 2014;569:80–4.
50. Ge Y, Wang L, Wang C, Chen J, Dai M, Yao S, et al. CX3CL1 inhibits NLRP3 inflammasome-induced microglial pyroptosis and improves neuronal function in mice with experimentally-induced ischemic stroke. Life Sci. 2022;300:120564.
51. Lee S, Xu G, Jay TR, Bhatta S, Kim KW, Jung S, et al. Opposing effects of membrane-anchored CX3CL1 on amyloid and tau pathologies via the p38 MAPK pathway. J Neurosci. 2014;34(37):12538–46.
52. Ahn JH, Kim DW, Park JH, Lee TK, Lee HA, Won MH, et al. Expression changes of CX3CL1 and CX3CR1 proteins in the hippocampal CA1 field of the gerbil following transient global cerebral ischemia. Int J Mol Med. 2019;44(3):939–48.
53. Wang J, Gan Y, Han P, Yin J, Liu Q, Ghanian S, et al. Ischemia-induced neuronal cell death is mediated by chemokine receptor CX3CR1. Sci Rep. 2018;8(1):556.
54. Zhang ZJ, Jiang BC, Gao YJ. Chemokines in neuron-glial cell interaction and pathogenesis of neuropathic pain. Cell Mol Life Sci. 2017;74(18):3275–91.
55. Kerkhofs D, van Hagen BT, Milanova IV, Schell KJ, van Essen H, Wijnands E, et al. Pharmacological depletion of microglia and perivascular macrophages prevents vascular cognitive impairment in Ang II-induced hypertension. Theranostics. 2020;10(21):9512–27.
56. Inoue K. Potential significance of CX3CR1 dynamics in stress resilience against neuronal disorders. Neural Regen Res. 2022;17(10):2153–6.
57. Kubíčková L, Dubový P. Dynamics of cellular regulation of Fractalkine/CX3CL1 and its receptor CX3CR1 in the rat trigeminal subnucleus caudalis after unilateral infraorbital nerve lesion-extended cellular signaling of the CX3CL1/CX3CR1 axis in the development of trigeminal neuropathic pain. Int J Mol Sci. 2024;25(11):6069.
58. Hulshof S, van Haastert ES, Kuipers HF, van den Elsen PJ, De Groot CJ, van der Valk P, et al. CX3CL1 and CX3CR1 expression in human brain tissue: noninflammatory control versus multiple sclerosis. J Neuropathol Exp Neurol. 2003;62(9):899–907.
59. Li Y, Zhang X, Cui L, Chen R, Zhang Y, Zhang C, et al. Salvianolic acids enhance cerebral angiogenesis and neurological recovery by activating JAK2/STAT3 signaling pathway after ischemic stroke in mice. J Neurochem. 2017;143(1):87–99.
60. Inose Y, Kato Y, Kitagawa K, Uchiyama S, Shibata N. Activated microglia in ischemic stroke penumbra upregulate MCP-1 and CCR2 expression in response to lysophosphatidylcholine derived from adjacent neurons and astrocytes. Neuropathology. 2015;35(3):209–23.
61. Tang Z, Gan Y, Liu Q, Yin JX, Liu Q, Shi J, et al. CX3CR1 deficiency suppresses activation and neurotoxicity of microglia/macrophage in experimental ischemic stroke. J Neuroinflammation. 2014;11:26.
62. Heinisch S, Kirby LG. Fractalkine/CX3CL1 enhances GABA synaptic activity at serotonin neurons in the rat dorsal raphe nucleus. Neuroscience. 2009;164(3):1210–23.
63. Deiva K, Geeraerts T, Salim H, Leclerc P, Héry C, Hugel B, et al. Fractalkine reduces N-methyl-d-aspartate-induced calcium flux and apoptosis in human neurons through extracellular signal-regulated kinase activation. Eur J Neurosci. 2004;20(12):3222–32.

Publisher's note